Design and development of a test method for the measurement of thermo-physical properties of different materials

Khan Z Ahmed 🆔, Mohammad Asif 🆔 and Mohammad Faizan

Abstract

The guarded hot plate method is widely used to measure the thermal conductivity and thermal resistance of materials having low thermal conductivity. An experimental set-up was designed and fabricated in-house to measure these properties. The set-up was built in accordance with ASTM D5470 standards. A novel insulating material waste tire rubber/polypropylene has been developed from the solid blend of waste tire rubber powder (425–300 μm) mixed with virgin polypropylene granules in a 2.5:1 ratio. The thermal conductivity of the newly developed insulating material in cylindrical solid form has been estimated. Further, thermal conductivity of a conducting material i.e., H-13 tool steel has been found out by using the present experimental set-up. In addition, the thermal contact conductance of a well-known thermal paste i.e., silicon grease has also been estimated for a range of temperatures and pressure using the present set-up. In the present study, the procedure for measuring thermal conductivity has been demonstrated along with the strengths and weaknesses of the experimental set-up and the suitability of the method for different materials. The experimental results reveal that the test method is equally suitable for the analysis of thermal interface material, and for measuring the thermal conductivity of solid specimens giving reliable results.

Introduction

The ability of a material to transfer heat from hot region to cold region through the material is referred to as thermal conductivity. It is usually denoted by the letter "k." Heat transfer in any material is based on three primary mechanisms, i.e., conduction, convection, and radiation, which may be acting alone or in combination. Generally, materials with high thermal conductivity are widely used for heat sink practices, and materials of low thermal conductivity are used for thermal insulations. The thermal conductivity through a material may be derived using Fourier's law of conduction. Thermal conductivity k under steady-state condition is given by the following expression.

$$Q = kA \frac{\Delta T}{\Delta x} \quad (1)$$

$$k = \frac{Q}{A} \times \frac{1}{\frac{\Delta T}{\Delta x}}$$

where Q is the rate of heat flow (W), k is the material's thermal conductivity (W/mK), A is area of cross-section (m^2) through which the heat flows, ΔT is the specimen's differential temperature and Δx is the test specimen's differential thickness (m).

Thus, the rate at which heat is transferred by conduction through a given unit area of a given material when the temperature gradient is normal to the area of cross-section can be termed as the thermal conductivity of the given material.[1,2] Temperature, elemental composition, size distribution, porosity, density, and the direction of the heat flow, all have a great impact on the material's thermal conductivity.[3–5]

The methods for measuring thermal conductivity that are available and commercialized are broadly divided into two types: Steady-state technique and transient techniques. Steady-state technique includes guarded hot plate apparatus (GHPA), radial heat flow technique, comparative method, parallel conductance technique, etc., whereas transient is largely Frequency-domain technique (3ω, frequency

Department of Mechanical Engineering, A.M.U, Aligarh, India

Corresponding author:
Khan Z Ahmed, Department of Mechanical Engineering, A.M.U, Aligarh, India.
Email: kzahir@myamu.ac.in

domain thermal reflectance, Pulse power method) and Time-domain technique (Hotwire technique, Laser flash technique, transient plane source (TPS) technique). Few of them are briefed in the following subsection.[6]

The thermal conductivity and thermal contact conductance (TCC) are evaluated in steady-state technique by measuring the temperature differential (ΔT) under a steady-state heat transfer (Q) through specimen.[7] The thermal conductivity can be determined by the slope of power against the temperature difference, steady-state technique is based on Fourier's law (1). This approach is suited for low thermal conductivity and structural components since they measure thermal conductivity directly. However, it takes a longer time than the transient technique to give results and needs large-size specimen.[8,9] It also has a disadvantage such as axial, radial heat losses, and contact resistance due to the usage of thermocouples/temperature sensors as the temperature sensors are used in the system.

Transient technique utilizes a heat source that is provided either regularly or as a flash, leading to a periodic signal (phase output signal) or transient temperature change (amplitude output signal) in the specimen.[9] This technique determines thermal diffusivity using a transitional heat flow during the heat treatment. Thermal diffusivity is a metric that quantifies the rate at which heat moves through a material. Its value is proportional to the specific heat capacity and density of the material as given by the equation below.[10]

$$\alpha = \frac{k}{\rho \, C_p} \qquad (2)$$

where α is the thermal diffusivity, ρ is the density of the specimen, k is the thermal conductivity, and C_p denotes the specific heat capacity.

The transient technique takes less time to give results (a few minutes), which minimizes the possibility of convection in fluid. Furthermore, thermal conductivity and thermal diffusivity are measured simultaneously. This can also work at high temperatures and pressures and uses small-size specimen. However, the accuracy of this technique is lower than steady-state technique.[11]

All of the techniques listed in Table 1 function in a specific range of temperatures and measure thermal conductivity up to a specified limit. TPS technique measure material's thermal conductivity from 0.001 to 1800 W/mK and have a wider thermal conductivity range. The transient hot wire and laser flash techniques are next, with measurements ranging from 0.005 to 500 W/mK and 0.1 to

1000 W/mK respectively. For testing range of temperature guarded hot plate, TPS and Laser flash technique are among top three with values ranging from −160 to 700 °C, −35 to 1000 °C, and −120 to 2800 °C, respectively. In addition, some researchers use other techniques to determine the k value of specimens, such as a differential photo-acoustic method being used for thin coating film,[12] a thermal wave method for thermal polymeric foils,[13] a photo-thermal deflection technique for anisotropy specimen[14] and a heated needling technique for plane shaped specimens.[15]

Xaman et al.[16] analyzed the temperature profile distribution for determining thermal conductivity. The Green's function formula was applied to determine the temperature profile in the guard plate and the center plate. When an analytical finding was matched to readings taken on aluminum plates, it was discovered that results are satisfactory when compared with the experimentally acquired data, with an acceptable error of 3%. Dubois et al.[17] validated GHPA for the estimation of thermal conductivity of crop-based insulation specimen and result was achieved with an accuracy of 2%. Similar results were reported by Salmon[18] who determined the thermal conductivity of insulating material using GHPA.

Alcocer[19] determined the thermal conductivity of various liquids like ethylene glycol, acetone, and deionized water by using the hot wire method. The error in the results is found to be less than 8% as validated by simulation and the results are in accordance with the other reported literature. Rouhani et al.[20] analyzed the thermal conductivity of low-grade heat adsorption thermal energy storage system. AQSOA FAM-Z02 packed bed adsorber of 2 mm diameter specimen with varying numbers of adsorbent sheets is evaluated under atmospheric condition and in 10–80 °C temperature range, error in results of thermal conductivity for room temperature and at 80 °C are 2% and 3%, respectively. Landa et al.[21] determined the thermal conductivity of refractory materials using the hot wire method. Researcher concluded the hot-wire approach may be utilized with an inaccuracy of around 10% for refractories with medium and low thermal conductivity (2–2.5 W/mK) for the temperature range 20–900 °C. The technique appears to be capable for evaluating k at high temperature upto 1400 °C.

The transient hot wire technique is one of the second most often utilized approaches around the world of thermal energy storage. Because of the adaptability of this approach, a wide range of materials and temperature range are available.[6] This technique collects over 100 data sets in 1 ms up to 1 s (10 s for solids). As a result, it can reach uncertainties of 1% for liquid, gas, solid and roughly ± 2% for nanofluid.[22] Alessandro Franco[23] determined the thermal conductivity of material for the construction industry using hot-wire technique. Materials having thermal conductivities ranging from 0.2 to 1.5 W/mK were found to have the best results. The accuracy of the results is well within 5% in good experimental conditions. Roder[24] studied fluid's thermal conductivity by using the transient hot-wire method. At real-time

Table 1. Variation in thermal conductivity of waste tire rubber/polypropylene (WTR/PP) solid blend.

Sr. No.	Sample	Thermal conductivity (W/mK)
I	WI	0.2436
2	W2	0.2311
3	W3	0.2458

rates of up to 1 s, data were measured with a platinum wire of 12.7 μm diameter. A computer system with a digital voltmeter is used in data acquisition system operated within temperature range of 70–320 K and pressure of 0–70 MPa. Results were obtained with accuracy of 1.5%. Similar results were reported by Richard et al.[25] for gases and liquids.

One commonly used technique to measure the thermal conductivity of material at laboratory scale is presented in ASTM D5470.[26] This test technique is used for measuring steady-state heat flux through the specimen. The calculations are done as though the specimen were homogeneous. However, in reality, these specimens are rarely homogeneous, although this supposition has no bearing on the utility of this test technique. This approach determines the contact thermal resistance and effective thermal conductivity of lubricants, thermally conductive compounds such as thermal interface materials, phase change materials, and solid materials. This technique has a limitation in that the thermal conductivity measurement at a very high temperature is challenging, and results are less reliable as maintaining proper insulation for repetitive experiments is a big challenge. The temperature gradient between two recorded temperatures is very minute and has a considerably large uncertainty.[27] The basic idea behind the procedure lies in the measurement of the temperature change in a layer of the specimen under test. The material whose thermal conductivity is to be found is kept between 2 cylindrical blocks of a material with a known and typically high thermal conductivity value. These blocks are known as Heat Flow Meter (HFM) blocks because of their role they perform in evaluating the thermal conductivity of the test specimen. One of these blocks is heated, while the other is cooled; this is done so that the temperature profile in the blocks, including the specimen material, is unidimensional and fixed in time.[28,29] The temperature gradient, and hence the heat flux passing through the blocks and the specimen material, can be found by evaluating the temperature profile in the axial direction of the two cylindrical blocks. Many thermocouples are placed along the length of the two cylindrical blocks and specimen material. The temperature data is obtained during the experiment by various thermocouples placed along the length of the cylindrical blocks. The thickness of the test specimen is set between the upper heat flow meter (UHFM) and the lower heat flow meter (LHFM). Based on the temperature data obtained along the length of test specimen and known thermal conductivity of the HFM cylindrical blocks, various parameters like heat flux through the specimen material, temperature change between UHFM and specimen material, relative heat flow resistance, the effective thermal conductivity of the specimen and TCC on the contact surface of specimen material and HFMs can be calculated. Thermal pastes are widely used in mobile, electronic part cooling applications to improve TCC at various interfaces for transferring heat from the power semiconductor unit to the heat sink. Thermal paste comprises conductive particulate, most commonly

metal oxides, embedded in a carrier material, most commonly silicon.[28,30,31]

This study aims to demonstrate the technique for measurement of the thermal conductivity (k) of a variety of materials ranging from insulating material, metals to thermal paste, and in accordance with ASTM D5470 standards. Experimental study of different specimens is performed using an apparatus designed and fabricated at the Department of Mechanical engineering of the Aligarh Muslim University in India. This article presents the thermo-physical findings and results of the tested specimens: A newly developed novel insulating material (waste tire rubber/polypropylene (WTR/PP) solid blend), H-13 tool steel, and silicon grease.

Temperature distribution calculation

The thermal conductivity through a specimen material may be derived using Fourier's law of heat conduction as given by the equation (1).

$$Q = kA \frac{\Delta T}{\Delta x}$$

Application of Fourier's law is essential regarding heat flux density which is directly proportional to the temperature gradient.[32,33]

$$\dot{q} \propto \nabla T; \dot{q} = -k\nabla T \tag{3}$$

Taking into consideration the assumptions of Fourier law, the differential equation is reduced to the following form

$$\frac{d^2 T}{dx^2} = 0; \frac{dT}{dx} = c; T(x) = C_1 x + C_2 \tag{4}$$

Since there is no heat generation within the system and material is assumed to be homogeneous and isentropic meaning that k value is constant in all the directions.

At the boundary conditions;

$$\text{at } x = 0, \ T = T_1 \ \text{and at } x = L, \ T = T_2 \tag{5}$$

where T_1, T_2 is the temperature at the edge of the specimen, solving the boundary conditions and equation (1), we get.

$$T(x) \frac{T_2 - T_1}{L} x + T_1 \tag{6}$$

As the temperature distribution is $y = mx + c$, it is a linear function, where $\frac{T_2 - T_1}{L}$ is the temperature gradient. Using temperature distribution equation and temperature gradient, the heat flux density $\dot{q}$ through the material can be evaluated.

$$\dot{q} = \frac{k}{L}(T_1 - T_2) \tag{7}$$

where, $\frac{k}{L}$ is the heat conduction resistance (R)

In the series-connected system where the density of heat flux passing through an arrangement of specimens

and cylindrical block can be derived by the following equation provided the temperatures T_1 and T_2 on the UHFM and LHFM surfaces are known.

$$\dot{q} = \frac{T_1 - T_2}{\dfrac{L_1}{k_1} + \dfrac{L_2}{k_2} + \dfrac{L_3}{k_3} + \ldots + \dfrac{L_n}{k_n}} = \frac{(T_1 - T_2)}{\sum_{i=1}^{n} \dfrac{L_i}{k_i}} \quad (8)$$

For the case of one-dimensional heat conduction through multiple layers (2 HFMs and 1 testing specimen) if the thermal conductivity of UHFM and LHFM is already known while the thermal conductivity of the test specimen k is not known, the equation (8) is reduced to the following form:

$$\dot{q} = \frac{T_1 - T_2}{\dfrac{L_1}{k_1} + R_{s1} + \dfrac{L}{k} + R_{s2} + \dfrac{L_2}{k_2}} = \frac{T_1 - T_2}{\dfrac{L_1}{k_1} + \dfrac{L}{k} + \dfrac{L_2}{k_2} + 2R} \quad (9)$$

whereas, all the values in equation (9) with subscripts 1 and 2 pertain to the values of UHFM and LHFM, respectively. Since the contact resistances R_{s1} and R_{s2} are the same because both the HFMs are of the same material and they have contact resistance with the testing specimen thus it is written as $2R$.

Once the value of k_1, k_2, and ΔT is known, then heat flux through UHFM and LHFM can be evaluated using the Fourier law. Finally, the average of the two of the $\dot{q}_1$ and $\dot{q}_2$ obtained for UHFM and LHFM blocks is used to measure the value of the heat flux flowing through the specimen material.

$$\dot{q}_{avg} = \frac{\dot{q}_1 + \dot{q}_2}{2} \quad (10)$$

Now, the temperature drop seen between the specimen material and UHFM, similarly, the temperature drop seen between the specimen and LHFM can be evaluated. Finally, the thermal resistance and thermal conductivity through the specimen can be calculated by the following expression.

$$R_{specimen} = \frac{\nabla T}{\dot{q}} \quad (11)$$

$$k_{specimen} = \frac{\dot{q}_{avg}}{\left(\dfrac{\Delta T}{\Delta x}\right)_{specimen}} \quad (12)$$

where $R_{specimen}$ denotes the thermal resistance, $k_{specimen}$ is the specimen's thermal conductivity. Using this steady-state method, the thermal conductivity and thermal resistance of the specimen material can be determined.

Materials and specimen preparation

In the present study, experiments were conducted on three different materials, i.e., a new insulating material (WTR/PP solid blend), H-13 tool steel, and a thermal paste silicon grease to analyze the thermal properties of the materials under a specific temperature and pressure range.

WTR/PP solid blend

WTR/PP solid blend ($\rho = 0.9456$ g/cm^3) is a mixture of waste tire rubber powder (425–300 µm) and virgin polypropylene granules in a 1:4 ratio blended in the single screw filament extruder machine at a temperature of 160 °C as the melting point of PP is around 160–170 °C. The molten matrix of WTR and PP is collected in a cylindrical tank with a diameter of 25 mm. The three solid cylindrical specimens of 15 mm height and 25 mm diameter (W_1, W_2, W_3) are developed for the tests. Holes of 2 mm diameter and 12.5 mm depth are drilled for the arrangement of thermocouples at an interval of 6 mm and 1.5 mm from the specimen ends as shown in Figure 1(a). It is well known that WTR ($k = 0.102$–0.32 W/mK) and PP material ($k = 0.15$–0.22 W/mK) are both insulating in nature with relatively low thermal conductivity, hence the newly developed material will also be an insulating material.

H-13 tool steel

A commercially produced H-13 tool steel ($\rho = 7.8$ g/cm^3) is chosen as a test specimen due to its extensive applications in manufacturing industries. H-13 tool steel test specimen was cut from a cylindrical rod and machined to a
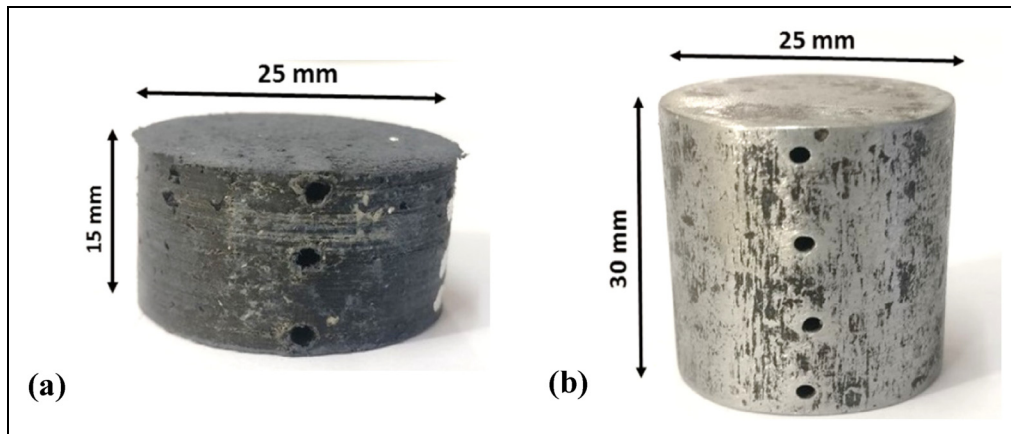

Figure 1. Pictorial view: (a) waste tire rubber/polypropylene (WTR/PP) solid blend; (b) H-13 tool steel specimen.

length of 30 mm and a diameter of 25 mm as shown in Figure 1(b). On both terminal faces, the specimen was nicely turned. To put the thermocouples, four holes of 12.5 mm depth and 2 mm diameter were bored into the specimen at an interval of 9 mm but 1.5 mm from the specimen ends, using vertical drilling machine-based manufacturing techniques.

Silicon grease (Thermal paste)

A commercially available thermal paste called silicon grease ($k = 0.7\,\mathrm{W\,/\,mK}$, $\rho = 1.03\,\mathrm{g/\,cm^3}$) was chosen to study TCC as it exhibits low volatility and high thermal stability at high temperatures. Silicon grease was applied between two stainless steel (SS) blocks as an interstitial material under varying temperature and loading conditions.

Experimental set-up

A simple experimental set-up with high quality, precise and well-calibrated devices has been designed and assembled in accordance with ASTM D5470 for the measurement of thermal conductivity and TCC. This set-up comprises of a cooling system, heating system, temperature measurement system, loading system, HFMs and insulation.

Components

The major components of the set-up are described as follows:

Cooling system. The cooling system design aims to generate a sufficient amount of total flow and distribute it effectively to keep the temperatures at the optimal level. A cooling system with a capacity equal to a heater serves our purpose. It consists of a fluid with high specific heat, so its temperature does not rise significantly along the passage. Another major part of a cooling system is a network of pipes providing an interface for heat transfer and a path for coolant. For efficient working of the cooling system inlet temperature of the fluid should be maintained at a constant value achieved by circulating the chilled water to extract its heat.

Conventional liquid cold plates on the market are usually basic geometry, such as a tube inserted in the base with two, four, or six passes. The drawback of these cold plates is that to get uniform flow across the whole base surface; we must increase the number of flow passes, which considerably increases the pressure drop. Therefore, a specially designed cylindrical block has been utilized for the cooling block, as shown in Figure 2. For efficient conduction of heat in the cooling system, copper is selected as the material of the cooling block.

The specifications of the cooling block are:

- Height: 25 mm.
- Diameter: 60 mm.
- Dimensions of the rectangular duct inside cooling block.
- Height: 11 mm, Width: 8 mm, Length: 50.26 mm.

A 26 mm grove with 3 mm depth is made on the top surface of the cooling block as a seat for the specimen. Two holes are made in the block, acting as the inlet and outlet for the cooling water circulation. Suitable attachments are provided to holes using air connectors to connect the chilled water circulation pipes.

Heating system. Two high-performance cartridge heater rods of 150 W each are inserted in a cylindrical shaped block made of copper to maintain a constant heat flux, resulting in high-temperature boundary conditions. The specially designed cores, stainless steel tubing, nickel–chromium resistance wire, careful selection of magnesium oxide fill, and carefully controlled production processes of the cartridge heater ensure high performance even under a harsh environment. The top surface acts as an insulating wall, whereas the bottom surface acts as a passage for
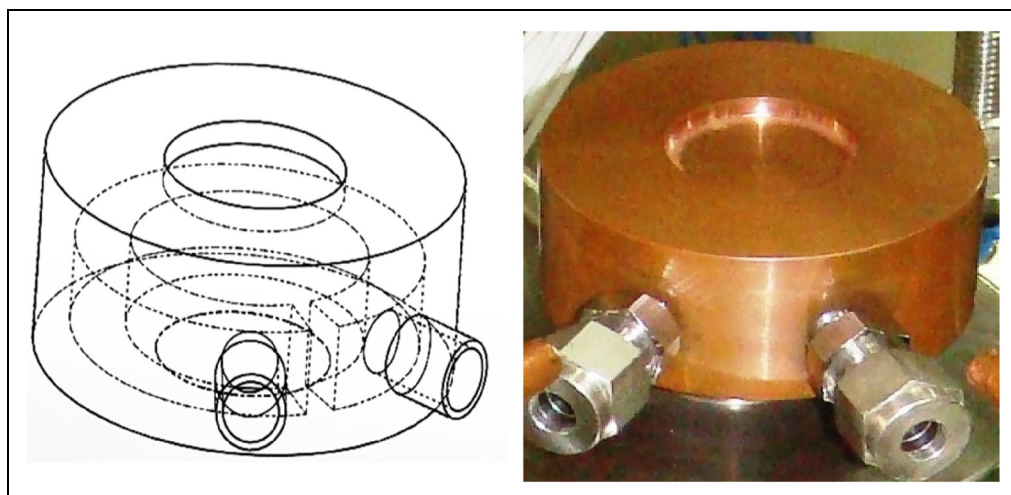

Figure 2. (a) Wireframe model of cooling block (b) Fabricated cooling block.

conduction. As the temperature profile inside the heating block is found to be uniform hence favorable towards providing constant wall temperature at the contact interface. The reason for favorable temperature profiles can be explained on the basis of lower localized heating due to the lesser accumulation of thermal energy. Heating rods are connected to a dimmerstat through a voltmeter and ammeter to provide a constant and measured heat supply.

Temperature measurement system. Copper constantan (T Type) thermocouples (diameter—0.5 mm) record the axial temperature data in the two specimens up to the steady-state, as shown in Figure 3. Small thermocouples are used to minimize conduction through the thermocouple leads. The thermocouples were all at least 1-meter long. The thermocouples were fixed in holes drilled perpendicular to the axis of specimen's symmetry. Each hole was approximately 12.5 mm deep, with a large diameter, enough to accommodate the thermocouple (about 2 mm). All the thermocouples are connected to a digital temperature indicator to record the temperatures up to the steady-state.

Loading system. Loading system mainly comprises of load applying mechanism and load measurement device. A screw jack of one Ton capacity has been used in the present experiment to apply the load to the test column to perform the experiments under varying contact pressure. A universal load cell of one Tonn capacity has been used to measure the load applied on the test column with the help of a screw jack. A load cell is connected to a digital indicator (LC = 0.1 kg) to display the load in kg.

Heat Flow Meter. Two cylinder blocks of known thermal conductivity are used as HFMs in the top and bottom of the specimen, i.e., UHFM and LHFM. HFMs are made of stainless steel 304 as its thermal conductivity is known with temperature as: $k(T) = 10.67 + 0.0159\,T$, where 'T' is in Kelvin.[34]

Insulations. To prevent axial heat loss, two nylon fiber insulating blocks are placed on top of the heating block just under the cooling block. Except for the cooling block, all the blocks were insulated with glass wool ($k = 0.023$ W/mK) with the critical insulation thickness (r_{cr}) of 10 mm to minimize the radial heat loss.

Limitations of the experimental set-up:

Geometry. The proposed setup is designed for a cylindrical shape specimen of a diameter of 25 mm and height of 100 mm approx. as the HFMs are of the cylindrical shape of the diameter of 25 mm. however, the specimen of the cuboidal shape of the diagonal length of 25 mm can also be tested.

Operating temperature. The specimen can be operated at a 5–200 °C temperature range. 5 °C on the cooling side and 200 °C on the heating side.

Time consumption. The proposed setup is based on the steady-state model, and the experiment is time-consuming as it takes up to 3 h to achieve the steady state.

Experimental procedure

All the blocks are thoroughly cleaned with acetone before use. It is essential for better heat transfer that the contacting surfaces are as conductive as possible then the heater, loading mechanism, and cooler have started to begin the heat flow across the test column and apply loads. The applied voltage is set as per the required operating temperature. After starting the heater and coolers, the set-up should be allowed to achieve steady-state heat transfer for around 120–180 min. In this experiment the heater is mounted at the very top followed by UHFM, specimen material, LHFM, and finally the cooling block. The glass-wool insulation was applied around the blocks. To record temperature data, a small gap was left so that thermocouples can be inserted as presented in Figure 3. Holes are created in the solid specimen material, whereas in case of thermal paste no such arrangement is needed. Two possible arrangements of HFMs and the specimen is demonstrated in the Figure 4. Load application is made using screw jack measured by load display unit. The temperature was recorded every 20 min till the change in temperature between current and previous readings was around 0.2 °C and the steady-state was achieved. This procedure is repeated by varying the load and changing the specimen.

Data analysis

Thermo-physical experimental data is collected for WTR/PP solid blend, H-13 tool steel, and Silicon grease. Firstly, the thermal conductivity of the solid specimens WTR/PP,
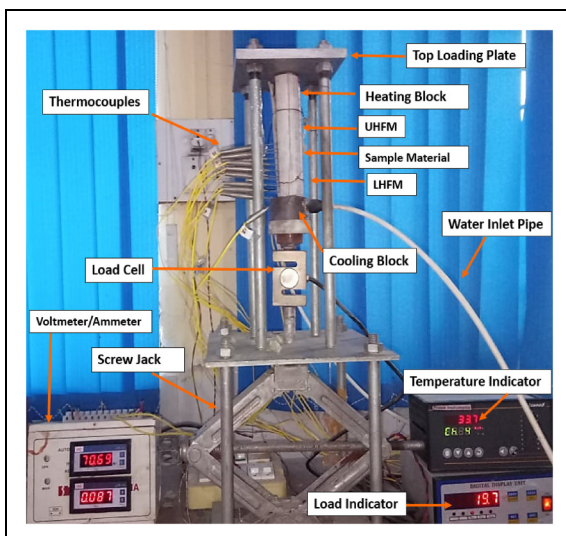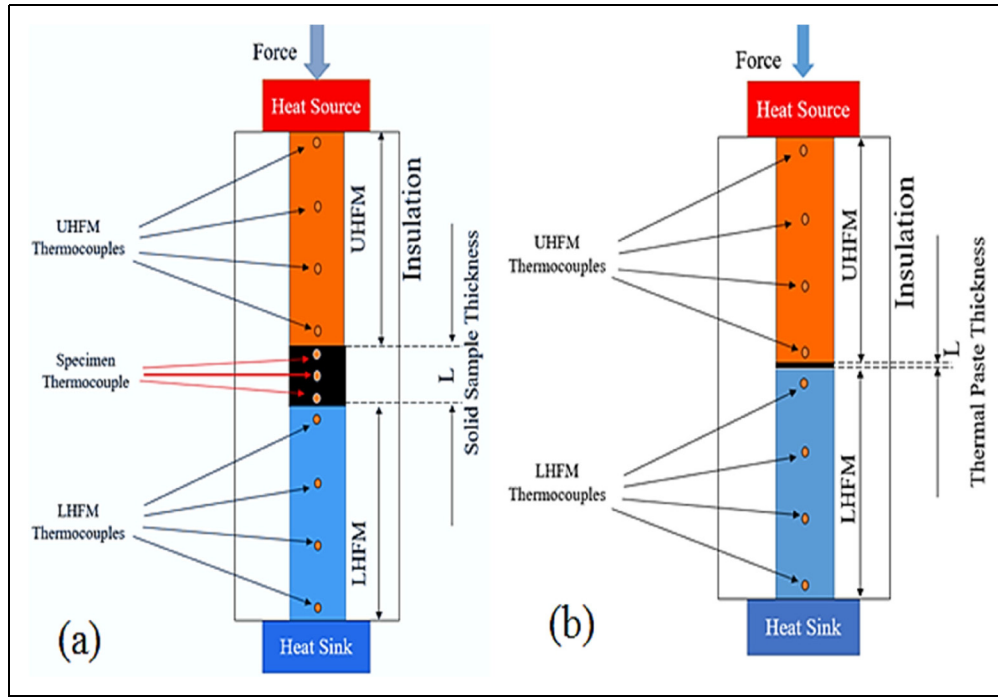

Figure 3. Experimental set-up.

Figure 4. Arrangement of specimen and HFMs: (a) for solid specimen; (b) for thermal paste.

H-13 tool steel is measured, silicon grease is applied on SS 304 pair and TCC is calculated under varying loading and temperature conditions.

Heat flux calculation

The temperature data at various locations of WTR/PP specimen, UHFM and LHFM is represented in a typical graph shown in Figure 5.

The temperature plot of the WTR/PP, UHFM and LHFM with respect to the thermocouple location is a linear function. Hence the temperature profile in the HFMs and specimen along its length may be linearly expressed as

$$y = mx + c$$

where y is the temperature, x is the distance along the line of specimen and HFMs and $m = \frac{\Delta T}{\Delta x}$

Heat flux can be evaluated by using the Fourier's law as $q = k \times \frac{\Delta T}{\Delta x}$

Estimation of thermal conductivity

The specimen with unknown thermal conductivity is placed between two stainless steel HFMs with known thermal conductivity. The thermal conductivity of the specimen is determined using the axial flow steady heat conduction technique. Thermocouples are employed to capture temperature profiles of HFMs and specimens at various locations (4 thermocouples on HFMs, 3 thermocouples on WTR/PP Solid, 4 thermocouples on H-13 tool steel). $\Delta T/\Delta x$ is calculated from temperature profile for HFMs and Specimen. The thermal conductivity
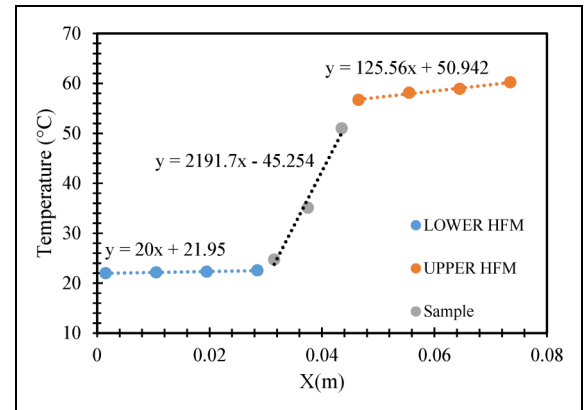

Figure 5. A typical plot of steady-state temperatures for LHFM, UHFM, and sample.
UHFM: upper heat flow meter; LHFM: lower heat flow meter.

data and temperature profile of two HFMs were utilized to determine the heat flux of HFMs ($\dot{q}_1$ and $\dot{q}_2$). The average heat flux ($\dot{q}_{avg}$) for UHFM and LHFM used for evaluation of thermal conductivity of specimen.

$$\dot{q}_{avg} = \frac{\dot{q}_1 + \dot{q}_2}{2}$$

Following Equation (12) has been used to evaluate the thermal conductivity of the specimen.

$$k_{specimen} = \frac{\dot{q}_{avg}}{\left(\frac{\Delta T}{\Delta x}\right)_{specimen}}$$

Estimation of TCC

The steady-state technique was used to calculate TCC. The steady-state technique is referred as an easy, efficient, and approved method for estimating TCC. In this method, temperature data from HFMs at various axial locations at steady-state is utilized. The average heat flux is calculated using the temperature profile in UHFM and LHFM as discussed earlier. Further, the drop in temperature at the interface is calculated by extrapolating the steady-state temperatures of the HFMs in contact using linear extrapolation.

Hence, TCC was calculated by the following equation:

$$\text{TCC} = \frac{\dot{q}_{avg}}{\Delta T}$$

where $\dot{q}_{avg}$ is the average heat flux and ΔT is temperature drop at the interface.

Uncertainty analysis

The most significant cause of uncertainty in evaluating thermal conductivity is based on the thermal conductivity of HFMs and specimen, heat flux measurement, temperature measurement, and thermocouple location. The uncertainty through each HFMs made of Stainless Steel is found to be 3.33%. All of the thermocouples used to measure temperature have been calibrated in the lab and are expected to be accurate to within 0.1 °C that results in 0.25%–0.5% uncertainty varying with temperature. However, the maximal inaccuracy in thermocouple hole depth is 0.1 mm in 12.5 mm depth, resulting in an error of 0.8%.

The following expression gives thermal conductivity, k under steady-state condition:

$$Q = kA\frac{\Delta T}{\Delta x}$$

$$k = \dot{Q} \times \frac{\Delta x}{\Delta T}$$

Finally, the overall uncertainty for the calculation of thermal conductivity may be stated as follows, according to the law of error propagation:

$$e_t = \frac{\delta k}{|k|} = \sqrt{\left(\frac{\delta(\dot{Q})}{\dot{Q}}\right)^2 + \left(\frac{\delta(\Delta T)}{\Delta T}\right)^2 + \left(\frac{\delta(\Delta x)}{\Delta x}\right)^2} \quad (13)$$

where $\frac{\delta(\dot{Q})}{\dot{Q}}$ is calculated for specimen and HFMs

$$\text{error \% in } \delta(\dot{Q}) = 3.33\%$$

Square sum of error % in $\delta(\dot{Q})$ is found to be 21.78% $\frac{\delta(\Delta T)}{\Delta T}$ and $\frac{\delta(\Delta x)}{\Delta x}$ is calculated for 11 thermocouples placed along the HFMs and specimen.

$$\text{error \% in } \Delta T = \frac{0.1}{20} \times 100$$

where 0.1 °C is the error of each thermocouple after calibration in laboratory and 20 °C is the minimum operating temperature. Error in ΔT is calculated for all the 11 thermocouples and its square sum is found to be 1.58%.

$$\text{error \% in } \Delta x = \frac{0.1}{x} \times 100$$

where 0.1 mm is displacement error in thermocouple location and x vary for each thermocouple. error in Δx is calculated for all the 11 thermocouples and its square sum is found to be 45.9874%.

Upon solving equation (13) with the available data, we get

$$e_t = \frac{\delta k}{|k|} = \sqrt{21.78 + 1.58 + 45.9874} = 8.327\%$$

therefore, experimental error comes out to be 8.327%. Similar findings are reported in the literature.[30]

Result and discussion

Thermo-physical property is dependent on various factors like pressure, working environment, and temperature etc. The findings discussed below were obtained during the experiments. Three different materials (insulating material, conducting material, and a thermal paste) were tested. Thermal conductivity of WTR/PP solid and H-13 tool steel while TCC of silicon grease with SS have been evaluated. The silicon grease is used as an interstitial material between metallic specimen of SS 304 with varying loading and temperature conditions. The results have been discussed in the following sub-sections:

WTR/PP solid (insulating material)

A new insulating material WTR/PP solid has been tested. Average Specimen Temperature was controlled by varying input heat flux to maintain the specimen approximately at 60 °C. A screw jack loading system is used to apply the load. The applied load had been kept constant as 10 kg to hold the HFMs and specimen material in the series array and to create proper contact between HFMs and the WTR/PP solid blend. A highly conductive thermal paste (graphene paste) was used between different interfaces of specimen and HFM to minimize the thermal contact resistance and improve heat transfer rate. Axial temperature data was recorded on the digital display unit against corresponding thermocouples till steady-state is achieved.

The recorded temperature data was used to calculate the heat flux of HFMs ($\dot{q}_1$, $\dot{q}_2$). The average of $\dot{q}_1$ and $\dot{q}_2$ was used to measure the heat flux flowing through the WTR/PP (1:4 ratio) solid blend using equation (10). The thermal conductivity value of three specimens of WTR/PP was calculated as 0.2436, 0.2311, and 0.2458 W/mK as presented in Table 1. The thermal conductivity results obtained for the WTR/PP material are satisfactory and in accordance with the thermal conductivity values for the similar composition material found in published literature.[35–38] Percentage Error in the thermal conductivity values of three specimens of WTR/PP is

found as 5.98%. This variation in thermal conductivity for the three specimens is due to small variations in composition caused due to manual feeding of WTR powder and PP granules in filament extruder machine during blending.

H-13 tool steel (conducting material)

H-13 tool steel specimen as shown in Figure 1(b) was tested at various temperatures 50, 80, 110, and 150 °C to study the thermal conductivity variation with temperature. The thermal conductivity was calculated and results were plotted as shown in Figure 6. As the alloy's temperature increases, the lattice vibration increases; thus, the thermal conductivity of the alloy is likely to increase.

As indicated by Figure 6, the thermal conductivity of H-13 tool steel increased with increasing temperatures. The thermal conductivity was found to be 35.6 W/mK at 50 °C which increases to 37.2 W/mK upon increasing temperature to 80 °C. The thermal conductivity upward trend
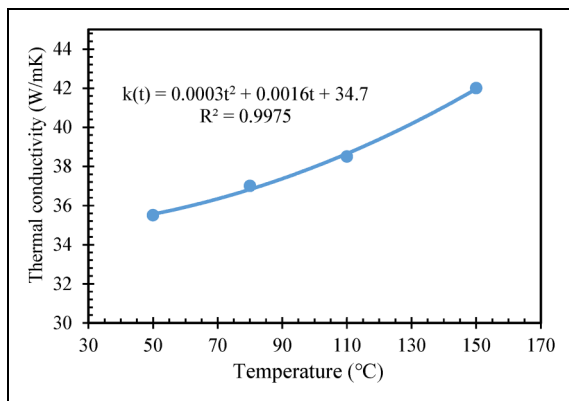
was followed for the temperature at 110 °C and 150 °C corresponding to 38.8 and 42 W/mK, respectively.

The thermal conductivity of the H-13 tool steel sample increased with increasing temperature over the entire temperature range studied and may be correlated with temperature as follows:

$$k(t) = 0.0003t^2 + 0.0016t + 34.7 \text{ with } R^2 = 0.9975$$

The thermal conductivity results obtained for the H-13 material are satisfactory and in accordance with the thermal conductivity values reported in published literature.[39,40]

Silicon grease (thermal paste)

Here, silicon grease (average thickness ≈ 30.5 μm) has been applied between the pair of SS 304 HFMs as a thermal interfacial material under varying heat input and loading conditions and TCC has been evaluated. Figure 7(a) presents the variation of TCC with contact pressure keeping constant input heat conditions (mean interface temperature (MIT) ≈ 50 °C). TCC for the stainless-steel pair with silicon grease as interstitial material has been found to be in the range of 5500–15500 for contact pressures ranging from 1 to 4 MPa. However, the TCC values of silicon grease presented by theoretical model in Yovanovich et al.[41] are little bit higher. It is due to heat loses in the thermal contacts during actually working conditions as against the ideal conditions in theoretical model of Yovanovich et al.[41] Further, the variation of TCC with MITs at constant pressure 4 MPa is shown in Figure 7(b). It has been noted that TCC continues to rise with increasing interface temperature. This might be attributed to temperature related changes in thermomechanical properties of interstitial material and specimens. The percentage change in TCC was found to be around 131% with an almost 42 °C temperature shift from 33 to 75 °C.
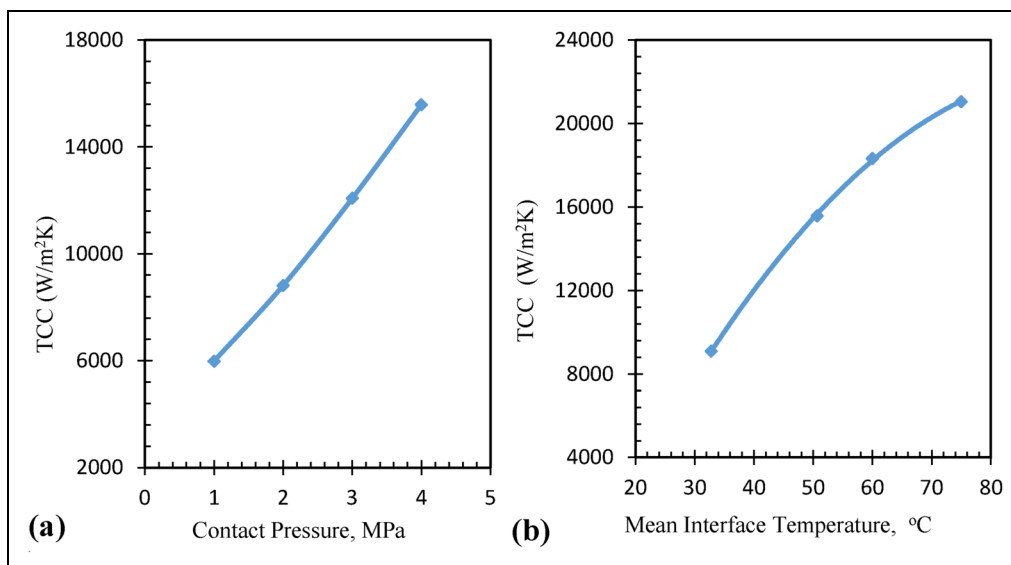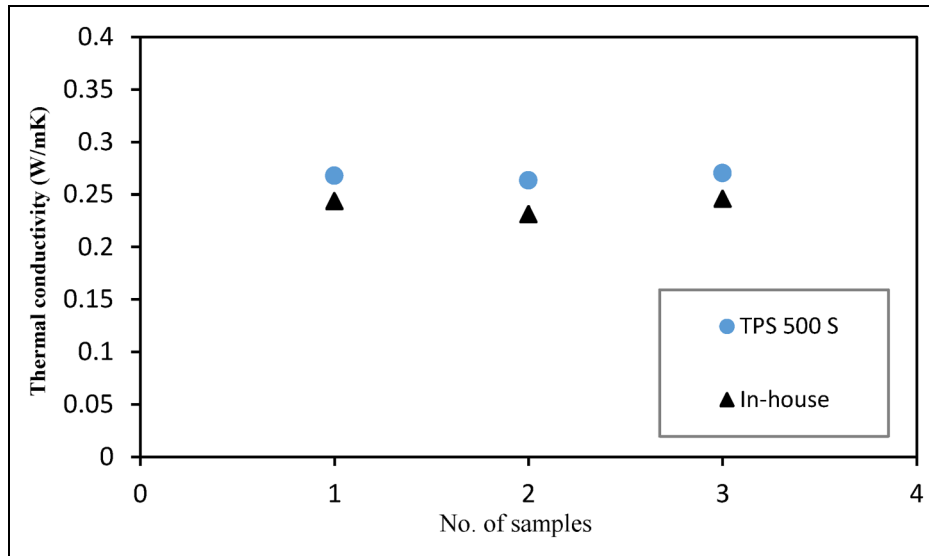

Figure 6. Thermal conductivity variation for H-13 tool steel with temperature.

Figure 7. Variation of TCC for silicon grease: (a) with contact pressure, (b) with mean interface temperature (MIT) at 4 MPa.

Table 2. Cost comparison with commercially available Set-up.[42–46]

Sr. No.	Model No.	Cost ($)	Temperature range	Geometry	Test range (W/mK)	Accuracy (%)
1	DRX-II-RL[42]	16,000	0–100 °C	Cylindrical shape	0.5–100	± 1–3
2	SKZ175C[43]	11,880	20–50 °C	Cuboidal shape	0–500	± 1
3	CY809-S[44]	8000	25–130 °C	Cuboidal shape	0.005–300	± 3
4	TPS 500 S[46]	40,000	Ambient	Cylindrical/Square/Rectangular	0.03–200	± 1
5	Self-designed	700	5–200 °C	Cylindrical shape	0.1–50	± 8–9

Figure 8. Thermal conductivity value comparison for waste tire rubber/polypropylene (WTR/PP) on different setups.

Comparison of in-house setup with commercially available setup

A cost comparison of in-house developed setup with various commercially available setup is performed and reported in Table 2. Furthermore, the absolute error between the in-house and commercially available setup (isotropic standard system TPS 500 S) is carried out for WTR/PP samples.

Absolute error between in-house developed setup and commercial setup (TPS 500 S). The thermal conductivity results were obtained and compared for three samples of WTR/PP (1:4 ratio) using a commercially available setup (TPS 500 S at IIT Kanpur) and an in-house developed setup. Deviation in the thermal conductivity value is presented in Figure 8. Absolute error is calculated as follows for the mean value of the WTR/PP's thermal conductivity.

$$\text{Absolute error} = \left| \frac{k\text{a} - k\text{b}}{k\text{a}} \right| \times 100$$

where

k_a is the thermal conductivity value of WTR/PP for in-house developed setup

k_b is the thermal conductivity value of WTR/PP for commercially available setup

$$\text{Absolute error}(\%) = \frac{0.2672 - 0.2401}{0.2672} \times 100$$

$$= 10.14\%$$

Cost comparison with commercially available apparatus. The above-mentioned self-designed apparatus costs approximately $700, which is inexpensive compared to other commercially available sophisticated set-ups. Table 2 shows that the present set-up is very affordable, with an extensive temperature range and a wide range of thermal conductivity measurements with reasonable accuracy. Therefore, it might be a viable option for determining thermo-physical properties.

Conclusion

In the present study, the application range and accuracy of thermal property measurements utilizing an in-house, self-fabricated but well-calibrated apparatus were investigated. Materials with thermal conductivities in the range of 0.1 W/mK to 50 W/mK were typically measured using steady-state technique based on the standard test method of ASTM D5470. An insulating material has been developed using waste tire rubber powder and virgin polypropylene granules. The thermal conductivity

of the new material and H-13 tool steel has been determined using the present experimental set-up. Moreover, the TCC of silicon grease between SS blocks has also been estimated for a range of temperatures and pressures. So, the apparatus had well enough capability to measure the thermo-physical properties for conducting materials, insulating materials, and thermal paste. However, material with very high conductivity and material with very low conductivity are challenging to work. It is noted that the exact measurement of the heat flux is difficult in the case of weak conductors whereas in case of high conducting material, precise measuring of temperature drop across the specimen is a challenge. Experimental results obtained are in accordance with the published values in literature with 8.327% experimental error. Hence, it is concluded that the present test set-up can be used to measure thermo-physical properties for a range of materials with reasonable accuracy.

Declaration of conflicting interests

Funding

ORCID iDs

Khan Z Ahmed https://orcid.org/0000-0002-9351-1453
Mohammad Asif https://orcid.org/0000-0002-6850-6820

References

1. Faheem A, Husain T, Hasan F, et al. Effect of nanoparticles in cutting fluid for structural machining of Inconel 718. *Adv Mater Process Technol* 2020; 8: 1–18.

2. Kakaç S, Yener Y and Naveira-Cotta CP. Foundations of heat transfer. *Heat Conduct* 2018; 5: 1–32.

3. Das R. Estimation of parameters in a fin with temperature-dependent thermal conductivity and radiation. *Proc IMechE, Part E: J Process Mechanical Engineering* 2016; 230: 474–485.

4. Ahmad S, Khan ZH, Zeb S, et al. Thermal and Entropy generation analysis of magnetohydrodynamic tangent hyperbolic slip flow towards a stretching sheet. *Proc IMechE, Part E: J Process Mechanical Engineering* 2021; 236: 357–367 DOI: 10.1177/09544089211041188.

5. Naveed M, Abbas Z and Imran M. Analytical simulation of time dependent electromagneto-hydrodynamic flow of Williamson fluid due to oscillatory curved convectively heated Riga surface with variable thermal conductivity and diffusivity. *Proc IMechE, Part E: J Process Mechanical Engineering* 2021; 236: 1–10. DOI: 10.1177/09544089211062357.

6. Zhao D, Qian X, Gu X, et al. Measurement Techniques for Thermal Conductivity and Interfacial Thermal Conductance of Bulk and Thin Film Materials. *J Electron Packag Trans ASME* 2016; 138: 1–19. DOI: 10.1115/1.4034605.

7. Raghuvanshi NS, Dutta G and Panda MK. Steady-state and nonlinear stability analysis for the feasibility of different fluids in a supercritical natural circulation loop. *Proc IMechE, Part E: J Process Mechanical Engineering* 2021; 236: 425–439. DOI: 10.1177/09544089211043970.

8. Manoj Praveen VJ, Vigneshkumar R, Karthikeyan N, et al. Heat transfer enhancement of air-concrete thermal energy storage system—CFD simulation and experimental validation under transient condition. *Proc IMechE, Part E: J Process Mechanical Engineering* 2021; 235: 1304–1314.

9. Xuan J, Zhou W, Song Y, et al. Improving the accuracy of the transient plane source method by correcting probe heat capacity and resistance influences. *Meas Sci Technol* 2013; 25: 015006.

10. Bamford M, Florian M, Vignoles GL, et al. Global and local characterization of the thermal diffusivities of SiCf/SiC composites with infrared thermography and flash method. *Compos Sci Technol* 2009; 69: 1131–1141.

11. Kishore V, Saxena NS, Saraswat VK, et al. Temperature dependence of effective thermal conductivity and effective thermal diffusivity of CdZnSe composite. *J Phys D Appl Phys* 2006; 39: 2592–2595.

12. Govorkov S, Ruderman W, Horn MW, et al. A new method for measuring thermal conductivity of thin films. *Rev Sci Instrum* 1998; 68: 3828.

13. Rantala J, Jaarinen J, Wei L, et al. A thermal wave technique to determine thermal diffusivities of polymer foils. *Rev Prog Quant Nondestruct Eval* 1991; 103: 2165–2172.

14. Jeon PS, Kim JH, Kim HJ, et al. Thermal conductivity measurement of anisotropic material using photothermal deflection method. *Thermochim Acta* 2008; 477: 32–37.

15. Ziouche K, Bougrioua Z, Lejeune P, et al. Probing technique for localized thermal conductivity measurement. *Meas Sci Technol* 2015; 26: 087003.

16. Xamán J, Lira L and Arce J. Analysis of the temperature distribution in a guarded hot plate apparatus for measuring thermal conductivity. *Appl Therm Eng* 2009; 29: 617–623.

17. Dubois S and Lebeau F. Design, construction and validation of a guarded hot plate apparatus for thermal conductivity measurement of high thickness crop-based specimens. *Mater Struct Constr* 2015; 48: 407–421.

18. Salmon D. Thermal conductivity of insulations using guarded hot plates, includingrecent developments and sources of reference materials. *Meas Sci Technol* 2001; 12: R89.

19. Alcocer G. Determination of the thermal conductivity by using the hot wire method: theory, simulation and experiment. *Mediterr J Basic Appl Sci* 2020; 04: 110–135.

20. Rouhani M, Huttema W and Bahrami M. Effective thermal conductivity of packed bed adsorbers: part 1 – experimental study. *Int J Heat Mass Transf* 2018; 123: 1204–1211.

21. Landa YA, Litovskii EY, Glazachev BS, et al. Hot-wire method of determining the thermal conductivity of refractory materials. *Refract* 1978; 19: 561–565. 1979 199.

22. Assael MJ, Antoniadis KD and Wakeham WA. Historical evolution of the transient hot-wire technique. *Int J Thermophys* 2010; 31: 1051–1072. 2010 316.

23. Franco A. An apparatus for the routine measurement of thermal conductivity of materials for building application based on a transient hot-wire method. *Appl Therm Eng* 2007; 27: 2495–2504.

24. Roder HM. A transient hot wire thermal conductivity apparatus for fluids. *J Res Natl Bur Stand (1934)* 1981; 86: 457.

25. Richard RG and Shankland IR. A transient hot-wire method for measuring the thermal conductivity of gases and liquids. *Int J Thermophys* 1989; 10: 673–686. 1989 103.

26. ASTM International. Standard test method for thermal transmission properties of thin thermally conductive solid electrical insulation material. *ASTM D5470*.

27. Buliński Z, Pawlak S, Krysiński T, et al. Application of the ASTM D5470 standard test method for thermal conductivity measurements of high thermal conductive materials. *J Achiev Mater Manuf Eng* 2019; 95: 57–63.

28. Asif M and Kumar A. Experimental study of thermal contact conductance for selected interstitial materials. *Lect Notes Mech Eng* 2021; 29: 309–318.

29. Asif M, Tariq A and Singh KM. Estimation of thermal contact conductance using transient approach with inverse heat conduction problem. *Heat Mass Transf und Stoffuebertragung* 2019; 55: 3243–3264.

30. Tariq A and Asif M. Experimental investigation of thermal contact conductance for nominally flat metallic contact. *Heat Mass Transf und Stoffuebertragung* 2016; 52: 291–307.

31. Asif M and Ahad MA. Experimental study of thermal contact conductance of tool-sample interface after heat treatment. *Lect Notes Mech Eng* 2021: 41–53.

32. Holman. *Heat Transfer*. 10th Edition. New York: McGraw-Hill, 2009.

33. Cengel YA and Boles MA. *Thermodynamics: An Engineering Approach*. 9th Edition. New York: McGraw-Hill, 2019.

34. McGee GR, Schankula MH and Yovanovich MM. Thermal resistance of cylinder-flat contacts: theoretical analysis and experimental verification of a line-contact model. *Nucl Eng Des* 1985; 86: 369–381.

35. Patti A and Acierno D. Thermal Conductivity of Polypropylene-Based Materials. *Polypropyl - Polym Charact Mech Therm Prop* 2019; 3: 1–20. DOI: 10.5772/INTECHOPEN.84477.

36. Xie X, Li D, Tsai TH, et al. Thermal conductivity, heat capacity, and elastic constants of water-soluble polymers and polymer blends. *Macromolecules* 2016; 49: 972–978.

37. Shao J and Zarling JP. Thermal conductivity of recycled tire rubber to be used as insulating fill beneath roadways. *Univ alaska Fairbanks, USA*, 1995-2.

38. Marie I. Thermal conductivity of hybrid recycled aggregate – Rubberized concrete. *Constr Build Mater* 2017; 133: 516–524.

39. Arrizubieta JI, Cortina M, Mendioroz A, et al. Thermal diffusivity measurement of laser-deposited AISI H13 tool steel and impact on cooling performance of hot stamping tools. *Metals (Basel)* 2020; 10: 1–13. DOI: 10.3390/met10010154.

40. Kabir IR, Yin D, Tamanna N, et al. Thermomechanical modelling of laser surface glazing for H13 tool steel. *Appl Phys A Mater Sci Process* 2018; 124: 1–9.

41. Yovanovich MM, Culham JR and Teertstra P. Calculating interface resistance. *Electron Cool* 1997; 3: 1–9.

42. Shanghai Goldsu Industrial Co., Ltd. Laboratory Equipment, Thermogravimetric Analyzer, https://gs-industrial.en.alibaba.com/(accessed 21 April 2022).

43. Potentiometric Titrator—Manufacturer and Supplier, Supplier, http://www.skzindustrial.com/ (accessed 21 April 2022).

44. Hunan Zhenhua Analysis Instrument Co., Ltd—instrument, tester, equipment, https://hunanzhenhua.en.ec21.com/ (accessed 21 April 2022).

45. Jinan Cyeeyo Instruments Co., Ltd—GwongWong.com, https://cyeeyoinstruments.gongwong.com/ (accessed 21 April 2022).

46. TPS 500 S—Instruments—Hot Disk. https://www.hotdiskinstruments.com/products-services/instruments/tps-500-s/ (accessed 28 October 2022).

Nomenclature

A	Surface area of the specimen (m^2)
C_1 and C_2	Constants of integration
k	Thermal conductivity (W/mK)
L	Thickness of specimen (m)
L_1, L_2	Thickness of UHFM, LHFM
$\dot{q}$	Heat Flux Density
$\dot{q}_1$	Heat Flux flowing through UHFM
$\dot{q}_2$	Heat Flux flowing through LHFM
Q	Heat transfer (W)
r_{cr}	Critical thickness of insulation
R	Heat conduction resistance of specimen material
R_{s1}	Heat conduction resistance between specimen and UHFM
R_{s2}	Heat conduction resistance between specimen and LHFM
$\frac{\Delta T}{\Delta x}$	Temperature gradient